THE JOURNAL OF BIOLOGICAL CHEMISTRY VOL. 286, NO. 19, pp. 16914–16928, May 13, 2011

Phosphorylation of Connexin 50 by Protein Kinase A Enhances Gap Junction and Hemichannel Function*[S]

Received for publication, January 4, 2011, and in revised form, March 11, 2011 Published, JBC Papers in Press, March 24, 2011, DOI 10.1074/jbc.M111.218735

Jialu Liu[‡1], **Jose F. Ek Vitorin**[§1], **Susan T. Weintraub**[‡], **Sumin Gu**[‡], **Qian Shi**[‡], **Janis M. Burt**[§], **and Jean X. Jiang**[‡2]

From the [‡]*Department of Biochemistry, University of Texas Health Science Center, San Antonio, Texas 78229 and the* [§]*Department of Physiology, University of Arizona, Tucson, Arizona 85724*

Phosphorylation of connexins is an important mechanism regulating gap junction channels. However, the role(s) of connexin (Cx) phosphorylation *in vivo* are largely unknown. Here, we showed by mass spectrometry that Ser-395 in the C terminus of chicken Cx50 was phosphorylated in the lens. Ser-395 is located within a PKA consensus site. Analyses of Cx50 phosphorylation by two-dimensional thin layer chromatography tryptic phosphopeptide profiles suggested that Ser-395 was targeted by PKA *in vivo*. PKA activation increased both gap junction dye coupling and hemichannel dye uptake in a manner not involving increases in total Cx50 expression or relocation to the cell surface or gap junctional plaques. Single channel recordings indicated PKA enhanced transitions between the closed and ~200-pS open state while simultaneously reducing transitions between this open state and a ~65-pS subconductance state. The mutation of Ser-395 to alanine significantly attenuated PKA-induced increases in dye coupling and uptake by Cx50. However, channel records indicated that phosphorylation at this site was unnecessary for enhanced transitions between the closed and ~200-pS conductance state. Together, these results suggest that Cx50 is phosphorylated *in vivo* by PKA at Ser-395 and that this event, although unnecessary for PKA-induced alterations in channel conductance, promotes increased dye permeability of Cx50 channels, which plays an important role in metabolic coupling and transport in lens fibers.

Gap junctions are clusters of transmembrane channels that connect the cytoplasm of two adjacent cells and allow small molecules ($M_r \leq 1$ kDa), such as ions, metabolites, and second messengers, to be directly exchanged between cells. In vertebrates, the structural units of gap junctions are a group of membrane proteins called connexins that contains over 20 members arranged in an overlapping, tissue-dependent expression pattern (1). All connexins have well conserved transmembrane domains and conserved extracellular loops. In contrast, the intracellular loops and C termini of connexins are variable. Most of the connexins are modified post-translationally by phosphorylation, primarily on serine residues in the C terminus (2, 3). Phosphorylation of connexins has been implicated in the regulation of gap junction intercellular communication at multiple stages of the connexin life cycle, such as intracellular trafficking, channel assembly, channel gating, internalization, and connexin degradation (4, 5).

As an avascular organ, the vertebrate lens depends on an extensive network of gap junction-mediated cell-cell communication for transparency and homeostasis. The lens contains an anterior epithelial cell layer and fiber cells that constitute the bulk of the organ. Three connexins have been identified in the vertebrate lens. Cx43[3] is mainly expressed in the anterior epithelial cells and in the lens bow region. When epithelial cells at the lens equator gradually differentiate into lens fibers, Cx43 expression in those cells is down-regulated and replaced by two other connexins, Cx50 and Cx46 (6).

All three lens connexins are phosphoproteins. Cx43, a well studied connexin, has been shown to be phosphorylated in the C-terminal region by several kinases, including PKA, PKC, p34(cdc2)/cyclin B kinase, casein kinase 1, MAPK, and v-Src kinase (2, 3). However, little is known about lens fiber connexins Cx50 and Cx46 regarding their specific phosphorylation sites, kinases involved, and corresponding regulatory roles. Previous studies indicated that PKC might be involved in the phosphorylation of chicken lens fiber Cx50 (formerly Cx45.6) (7). Casein kinase 1 is responsible for the phosphorylation of ovine Cx50, which lowers the level of intercellular communication (8, 9). Our previous studies have shown that chicken Cx50 is phosphorylated *in vivo* by casein kinase II at Ser-364, which is located within a PEST domain of the C-terminal region (10). This phosphorylation not only facilitates the turnover of Cx50 but also prevents caspase-3-mediated cleavage in the C terminus during lens development (11). Chicken Cx46 (formerly Cx56) was shown to be phosphorylated at Ser-118 and Ser-493 in lens cell primary cultures. Activation of PKC led to an increase in the phosphorylation of Ser-118 and a reduction in the intercellular communication in a PKCγ-dependent manner (12). Recently, multiple *in vivo* phosphorylation and truncation sites of bovine Cx50 and Cx46 were identified by mass spectrometry (13, 14). Most of these identified phosphorylation sites were located on serine residues in the cytoplasmic C terminus. However, the corresponding kinase(s) involved and the functional importance of each of these phosphorylations have not been elucidated.

* This work was supported, in whole or in part, by National Institutes of Health Grant EY012085 (to J. X. J.). This work was also supported by Welch Foundation Grant AQ-1507 (to J. X. J.).

[S] The on-line version of this article (available at http://www.jbc.org) contains supplemental Figs. S1–S6.

[1] Both authors contributed equally to this work.

[2] To whom correspondence should be addressed: Dept. of Biochemistry, University of Texas Health Science Center, 7703 Floyd Curl Dr., San Antonio, TX 78229-3900. Fax: 210-567-6595; E-mail: jiangj@uthscsa.edu.

[3] The abbreviations used are: Cx, connexin; LY, Lucifer yellow; RD, rhodamine dextran; CEF, chicken embryonic fibroblast; UTHSCSA, University of Texas Health Science Center at San Antonio; TPCK, L-1-tosylamido-2-phenylethyl chloromethyl ketone or tosylphenylalanyl chloromethyl ketone.

In this study, we show that Cx50 in the chick lens is phosphorylated *in vivo* by PKA at Ser-395, which is a highly conserved amino acid residue across different animal species. PKA activation enhanced both Cx50 gap junction and hemichannel functions. Enhanced communication did not involve enhanced trafficking of Cx50 to the cell surface, increased Cx50 expression level, or increased gap junction plaque formation but did appear to involve stabilization of the channel in a more conductive configuration. Mutation of Ser-395 to alanine attenuated the PKA-mediated increase in communication and altered, but did not eliminate, the response of the channel to PKA. Together, these results suggest that phosphorylation by PKA plays an important role in promoting increased permeability of Cx50-comprised gap junctions and hemichannels in the lens cells.

EXPERIMENTAL PROCEDURES

Materials—Fertilized, unincubated eggs from white leghorn chickens were purchased from Ideal Poultry (Cameron, TX) and incubated in a humidified 37 °C incubator. 3000 Ci/mmol [γ-^{32}P]ATP and 0.4 mCi/ml $H_3[^{32}P]O_4$ were obtained from PerkinElmer NEN Radiochemicals (Waltham, MA). TPCK-treated trypsin, polyvinylpyrrolidone-360, anti-FLAG M2 monoclonal antibody, 8-Br-cAMP, forskolin, and PKA inhibitor (14–22) were purchased from Sigma. The catalytic subunit of cAMP-dependent PKA was from New England Biolabs (Ipswich, MA). Bicinchoninic acid microprotein assay kit, EZ-link Sulfo-NHS-LC-Biotin, and avidin beads were from Pierce. Ultrafree-MC centrifugal filter unit and C18-ZipTips were from Millipore (Bedford, MA). Trypsin, phosphate-free DMEM, and tissue culture reagents Lucifer yellow (LY) and rhodamine dextran (RD) were obtained from Invitrogen. PVDF membrane and Bio-safe colloidal Coomassie Blue G-250 were from Bio-Rad. QuikChange site-directed mutagenesis kit was from Stratagene (La Jolla, CA). FBS and dialyzed FBS were obtained from Hyclone Laboratories (Logan, UT). Cellulose TLC glass plates were from EMD Chemicals (Gibbstown, NJ). All other chemicals were obtained from either Sigma or Fisher.

Identification of Cx50 Phosphorylation Sites by HPLC-Electrospray Ionization-Tandem Mass Spectrometry—Approximately 400 embryonic day 18 chick lenses were collected immediately after sacrifice and rinsed three times in PBS. Crude lens membranes were prepared based on a previously described procedure with some modifications (10). Briefly, chick lenses were lysed and pelleted at 100,000 × *g* for 30 min at 4 °C. Immunoprecipitation was performed with affinity-purified anti-Cx50 antibodies covalently conjugated to protein A-Sepharose through a chemical cross-linker, dimethyl pimelimidate. Immunoprecipitation samples were concentrated through Ultrafree-MC centrifugal filter units (30,000 NMWL), fractionated by 12% SDS-PAGE, and visualized with Bio-Safe colloidal Coomassie Blue G-250. Gel-purified Cx50 bands were excised and digested *in situ* overnight in polypropylene tubes at 37 °C with modified trypsin (Promega) at an approximate ratio of 10:1 (protein:enzyme). The digests were analyzed by capillary HPLC-electrospray ionization-MS/MS on a Thermo Fisher LCQ Classic ion trap mass spectrometer in conjunction with a Michrom BioResources Paradigm MS4 micro HPLC and a home-built nanospray interface. On-line separation of tryptic peptides was conducted as follows: column, New Objective PicoFrit, 75 μm ID, packed to 10 cm with C18 Vydac 218MSB5 resin; mobile phase A, 0.5% acetic acid, 0.005% TFA in water; mobile phase B, 90% acetonitrile, 0.5% acetic acid, 0.005% TFA in water; gradient, 2% B to 72% B in 30 min; flow rate, 0.4 μl/min. Data-dependent acquisition was employed in which a survey scan was acquired followed by collision-induced dissociation spectra of the four most abundant ions in the survey scan. The uninterpreted tandem mass spectra were searched against the NCBInr data base by means of Mascot (Matrix Science). Assignments of tandem MS fragments were verified by comparison with theoretical patterns generated by GPMAW (Lighthouse Data).

In Vitro Phosphorylation by PKA—GST fusion proteins containing a partial C-terminal region of Cx50 (small fragment of Cx50 (Cx50FS), residues 369–400) and its corresponding point mutations, Cx50FS(S387A), Cx50FS(S395A), and Cx50FS(S387A,S395A) were expressed in *Escherichia coli* and purified by binding to glutathione-coupled agarose beads based on published procedures (15). Equal amounts of fusion proteins (2–4 μg of protein/reaction) were incubated with 3000 Ci/mmol [γ-^{32}P]ATP in PKA reaction buffer (50 mM Tris-HCl, pH 7.5, 10 mM $MgCl_2$, 200 μM ATP) for 30 min at 30 °C in the presence of 5,000 units of purified, catalytic subunit of PKA. The reactions were terminated by addition of SDS sample loading buffer and separated on 12% SDS-PAGE gels. Proteins resolved by SDS-PAGE were blotted onto nitrocellulose membranes (0.45-μm pore size) for autoradiography.

^{32}P Labeling of Chick Embryonic Lens Organs—^{32}P labeling of chick embryonic lens organs was conducted based on our previous protocol (7). Briefly, intact lenses were dissected immediately from embryonic day 10 chick embryos after sacrifice and washed three times with phosphate-free DMEM. The lenses were first incubated with phosphate-free DMEM with 5% dialyzed fetal bovine serum plus 1% L-glutamine for 30 min to reduce intracellular phosphate levels. The lenses were then labeled overnight in the same medium supplemented with 0.4 mCi/ml $H_3[^{32}P]O_4$. Immunoprecipitated Cx50 samples from ^{32}P-labeled lens organs were separated on 12% SDS-PAGE and subjected to two-dimensional tryptic phosphopeptide mapping analysis.

Two-dimensional Tryptic Phosphopeptide Analysis—Two-dimensional tryptic phosphopeptide mapping was performed based on published procedures with some modifications (10). Briefly, Cx50 C-terminal fusion proteins phosphorylated *in vitro* and immunoprecipitated Cx50 samples from ^{32}P-labeled lens organs were applied to 12% SDS-PAGE and blotted onto nitrocellulose membranes for autoradiography. Phosphorylated protein bands were excised from membranes and cut into small pieces. The strips of membrane were soaked for 30 min at 37 °C in 0.5% polyvinylpyrrolidone-360 in 100 mM acetic acid and extensively washed with deionized water. The samples were then digested with TPCK-treated trypsin at 37 °C overnight. The tryptic phosphopeptides were first concentrated, then desalted on C18-ZipTips, and resolved on two-dimensional TLC plates by electrophoresis in running buffer (2.5% formic acid, 7.5% acetic acid, 90% deionized water, pH 1.9) at

1.0 kV for 30 min for the first dimension and by ascending chromatography orthogonal to the first dimension in TLC chromatography buffer (37.5% *n*-butanol, 25% pyridine, 7.5% acetic acid, 30% deionized water) for the second dimension. The plates were exposed to x-ray film in the presence of an intensifying screen at −70 °C for autoradiography.

Preparation of Recombinant Retroviral Constructs and High Titer Retroviruses Containing Wild-type and Mutant Cx50—Retroviral constructs and high titer retroviruses were prepared based on our previous protocol (16). Briefly, a cDNA fragment containing the C-terminal FLAG-tagged wild-type Cx50 was generated by polymerase chain reaction and subcloned into an adapter vector, Cla12NCO, and then inserted into a retroviral vector *RCAS*(*A*). High titer recombinant retroviruses expressing wild-type Cx50 were generated through transfection in chicken embryonic fibroblast (CEF) cells ($1–5 \times 10^8$ colony-forming units/ml). For expression in the connexin-deficient, Rin (tumorigenic rat insulinoma) cells, wild-type Cx50 were subcloned into the EcoRI site of the pIRES2-EGFP expression vector. Using wild-type Cx50 DNA construct as a template, Cx50(S395A) and Cx50(S387A,S395A) mutants containing corresponding point mutations were generated using the QuikChange™ site-directed mutagenesis kit according to the manufacturer's instructions. The codons encoding Ser-395 (TCA) and Ser-387 (AGT) were changed to GCA and GCT, respectively, which encode Ala. PCR primers required for generation of these mutants were synthesized at the University of Texas Health Science Center (UTHSCSA) DNA Core Facility. All of the constructs generated were sequenced at the UTHSCSA DNA Core Facility to ensure that the correct sequences were present.

Preparation of Embryonic Lens Primary Cultures—Embryonic lens primary cultures were prepared following a modified procedure described previously (17). Briefly, lenses dissected from 11-day-old chick embryos were washed with TD buffer containing 140 mM NaCl, 5 mM KCl, 0.7 mM Na_2HPO_4, 5 mM glucose, and 25 mM Tris (pH 7.4) and digested with 0.1% trypsin in TD buffer at 37 °C. The lenses were then broken apart by pipetting up and down in M199 medium plus 10% FBS and 1% penicillin/streptomycin. The cells were collected and resuspended in M199 medium. Living cells were then counted and seeded at 4×10^6 cells/35-mm tissue culture plate. The cultures were incubated at 37 °C, 5% CO_2 and fed every other day. Scrape loading dye transfer was performed when the cells became 90% confluent (after ~4 days) and started to form lens fiber-like "lentoid" structures.

Scrape Loading Dye Transfer Assay—Connexin-deficient CEF cells expressing exogenous Cx50, Cx50(S395A), or Cx50(S387A,S395A) mutant by retroviral infection were grown to confluence to maximize contact among cells. Scrape loading dye transfer assays were performed based on a published procedure (18) with some modifications. Briefly, after three washes with Hanks' balanced salt solution plus 1% BSA for 5 min each, the cells were scraped lightly with a 26.5-gauge needle in 1% LY, 1% RD in PBS. LY (molecular mass, 457 Da) can pass through gap junction channels, whereas RD (molecular mass, 10 kDa) is too large to pass. Therefore, the presence of LY indicates cells participating in gap junction-mediated communication and RD serves as a tracer dye for cells originally receiving the dyes. After incubation for 15 min, the cells were washed with HBSS three times and twice with PBS and then fixed in fresh 2% paraformaldehyde for 30 min. Dye transfer results were examined using a fluorescence microscope (Zeiss) in which LY and RD could be detected by using fluorescein and RD filters, respectively. Acquisition conditions were kept consistent for all measurements, and no threshold adjustments were used. The extent of dye transfer was quantified by measuring the ratio of LY transfer distance from scrape lines to RD transfer distance. A minimum of five images per condition tested with six measurements per image were used to assess the extent of dye transfer.

Dye Uptake Assay—Dye uptake analysis was performed as previously described (19) with some modifications. Briefly, CEF cells expressing exogenous Cx50, Cx50(S395A), or Cx50(S387A,S395A) by retroviral infection were grown at low cell density to ensure no physical contact among the majority of cells. LY was used as a tracer for measuring hemichannel activity, with RD as a negative control. The cells were mechanically stimulated to open hemichannels by dropping Ca^{2+}-free minimum essential medium from a pipette at a fixed distance. The cells were then incubated in the presence of 0.4% LY, 0.4% RD for 5 min, and the cells were washed with medium containing 1.8 mM Ca^{2+} and then fixed with 1% PFA. Similar fields were observed under the fluorescence microscope. Dye uptake was presented as a percentage of fluorescent cells divided by the total number of cells.

Culture of CEF Cells, Retroviral Expression, and Preparation of Cell Membranes—CEF cells were seeded at 2.5×10^5 cells in 60-mm tissue culture plates with DMEM plus 10% fetal calf serum, 2% chicken serum, and 5% CO_2. The cells were infected on the second day with high titer retroviruses ($1–5 \times 10^8$ colony-forming units/ml). After reaching confluence, CEF cells were digested with 0.05% trypsin and plated into 60- or 100-mm culture plates. At confluence, the cells were collected and lysed in ice-cold lysis buffer (5 mM Tris, pH 8.0, and 5 mM EDTA/EGTA) plus 2 mM phenylmethylsulfonyl fluoride, 10 mM *N*-ethylmaleimide, and 100 μM leupeptin through a 26.5-gauge needle. The cell lysates were then centrifuged for 5 min at $1000 \times g$ to remove cell debris. Crude membranes were pelleted at $100{,}000 \times g$ for 30 min (TLA-100.3 rotor, Beckman) and resuspended in lysis buffer.

SDS Gel Electrophoresis, Radiography, and Western Blot Analysis—Crude membrane extracts resuspended in lysis buffer were boiled in 0.6% SDS for 3 min, and then the proteins were separated by 10% SDS-PAGE. Gels loaded with ^{32}P-labeled samples were blotted onto nitrocellulose membranes for autoradiography. Western blots were performed by probing with anti-FLAG (1:1000 dilution) and anti-β-actin (1:5000 dilution). Primary antibodies were detected with horseradish peroxidase-conjugated goat anti-rabbit IgG (1:5000 dilution) or anti-mouse IgG (1:5000 dilution) using chemiluminescence reagent kit. The intensities of the bands on Western blots were quantified by densitometry.

Cell Surface Biotinylation—Biotinylation of monolayered cells was performed based on a procedure described previously (20) with some modifications. Briefly, CEF cells expressing exogenous Cx50, Cx50(S395A), or Cx50(S387A,S395A) by ret-

roviral infection were labeled with 0.5 mg/ml EZ-link Sulfo-NHS-LC-Biotin in PBS at 4 °C for 30 min. The cells were washed three times with PBS containing Ca^{2+}, Mg^{2+}, and glycine and lysed in radioimmune precipitation assay buffer (25 mM Tris-Cl, 100 mM NaCl, 1 mM EDTA) plus 1% sodium deoxycholate, 1% Triton X-100, 0.1% SDS, and protease inhibitors. The cell lysates were mixed with equal volumes of neutravidin beads and incubated at 4 °C overnight. The beads were then washed five times with PBS until no proteins could be detected in the elute by measurement of spectrometric absorbance at 280 nm. The biotinylated proteins were eluted by boiling for 5 min in sample loading buffer containing 1% SDS and 2% β-mercaptoethanol, and equal volumes of each sample were loaded on SDS-PAGE and analyzed by Western blotting using monoclonal anti-FLAG or anti-β-actin antibody. The intensities of protein bands were quantified by densitometry (Image J software; National Institutes of Health), and the ratios of biotinylated sample to total lysate were obtained.

Extraction of Detergent-resistant Gap Junctional Plaques—Preparation of gap junction plaques was performed based on a published method (21) with some modifications. Briefly, CEF cells expressing exogenous Cx50 by retroviral infection were treated in the absence and presence of forskolin or 8-Br-cAMP. Crude membrane samples prepared from cell lysates were mixed and incubated with 1% Triton X-100 on ice for 30 min and centrifuged at 140,000 × *g* for 30 min at 4 °C. After collecting the supernatant, the pellet not solubilized in Triton X-100 was resuspended in lysis buffer containing 1% SDS.

Immunofluorescence—Immunofluorescence staining of CEF cells treated with forskolin or 8-Br-cAMP was performed on glass coverslips using affinity purified anti-Cx50 antibody (1:500 dilution) and followed by the incubation with FITC-conjugated anti-rabbit IgG secondary antibody. DAPI was used to label the nuclei. The cells were visualized using confocal laser scanning microscopy (Fluoview; Olympus Optical, Tokyo, Japan) at the Imaging Core facility (UTHSCSA).

Channel Electrophysiology—Rin cells were transfected with Cx50 or Cx50(S395A) using the pIRES-eGFP vector and Lipofectamine; 24–36 h after transfection, the cells were plated on glass coverslips and maintained continuously under selective pressure (G418 300–400 μg/ml). Transfection efficiency and resultant levels of coupling were comparable for wild-type and mutant proteins (supplemental Fig. S1, *A* and *B*). Channel activity was studied 3–7 days later, when gap junction coupling was readily detected (supplemental Fig. S1*C*). Dual whole cell voltage clamp recordings of channel activity were performed as previously described (22) on cells treated or not with 8-Br-cAMP (final concentration, 0.5–1.0 mM; although a few experiments with similar results were obtained in 50 μM 8-Br-cAMP). Halothane (up to 8 mM) was added to the external solution as necessary to reveal the activity of individual channels. Channel activity was digitally recorded and analyzed manually using pClamp8 (Axon/Molecular Devices), Excel (Microsoft), Origin (OriginLab Corp.), and SigmaPlot (SPSS Inc.) software as appropriate. The amplitudes of transitions separating transjunctional current levels that were within 25 pA of base line and stable for 100 ms before and after the transition were measured. Transitions away from (opening events) and toward (closing events) base line were evaluated; transitions possibly involving nonunitary events were excluded. Current amplitudes divided by the transjunctional voltage gradient (±40 mV) yielded the conductances of transitions ($\gamma_j = I_j/V_j$). All points and channel transition histograms were then constructed as usual. Channel open time was estimated by measuring elapsed time between opening transitions and the next closing transitions; these measures were compiled as frequency open time histograms. Open time data were further segregated by their corresponding transition amplitudes. Transition amplitude and open time frequency histograms were best fit with Gaussian or exponential decay functions, as appropriate, for comparison.

Statistical Analysis—Unless otherwise stated, data were analyzed with one-way analysis of variance and Newmann-Keul's multiple comparison test via GraphPad Prism (GraphPad Software, La Jolla, CA). The data are presented as the means ± S.E. of multiple measurements. The *asterisks* in the figures represent the degree of significance in comparison with controls (*, $p < 0.05$; **, $p < 0.01$; ***, $p < 0.001$). Some of the data presented were normalized to controls for comparison.

RESULTS

Identification of Ser-395 as a Highly Conserved Phosphorylation Site of Cx50 in Vivo—To identify the *in vivo* phosphorylation sites on Cx50, we first isolated the Cx50 protein from embryonic chick lenses by immunoprecipitation followed by one-dimensional SDS-PAGE and then analyzed the tryptic digest of the purified sample by HPLC-electrospray ionization-MS/MS. Fig. 1*A* shows the tandem mass spectrum of the ion at *m*/*z* 478.8 (2+) assigned with ≥95% confidence as ARpSDDLTV (pS395). The ion at *m*/*z* 429.1 corresponds to a fragment generated by the neutral loss of H_3PO_4 (−98 Da), characteristic of a phosphopeptide. The observed b-fragment (N-terminal) and y-fragment (C-terminal) ions allowed unambiguous localization of phosphorylation at Ser-395 for chicken Cx50.

Sequence analysis showed that the last 30 amino acid residues in the C terminus of Cx50, including Ser-395, are highly conserved across animal species, such as human, rat, mouse, ovine, bovine, and chicken (Fig. 1*B*). Consensus phosphorylation sequence analysis performed using the NetPhosK 1.0 prediction server (Center for Biological Sequence Analysis, Technical University of Denmark, Iyngby, Denmark) indicated that PKA is the predicted kinase responsible for Ser-395 phosphorylation. Ser-387 in the C terminus of Cx50 was identified as another putative consensus site for PKA phosphorylation (Fig. 2*C*). However, the output probability score (value in the range 0.00–1.00) of Ser-387 (score, 0.54) is much lower than that of Ser-395 (score, 0.71).

Cx50 Is Phosphorylated at Ser-395 by PKA in the Lens in Vivo—To determine whether Ser-395 can be phosphorylated by PKA *in vitro*, a GST-tagged Cx50 C terminus construct and mutants Cx50FS(S395A), Cx50FS(S387A), and Cx50FS(S387A,S395A) were generated (Fig. 2*A*). GST-tagged Cx50 C terminus fusion proteins were purified and resolved by SDS-PAGE (Fig. 2*B*). Interestingly, all GST-tagged Cx50FS fusion proteins migrated as doublet bands on SDS-PAGE, with an apparent molecular mass of close to 29 kDa. The separation

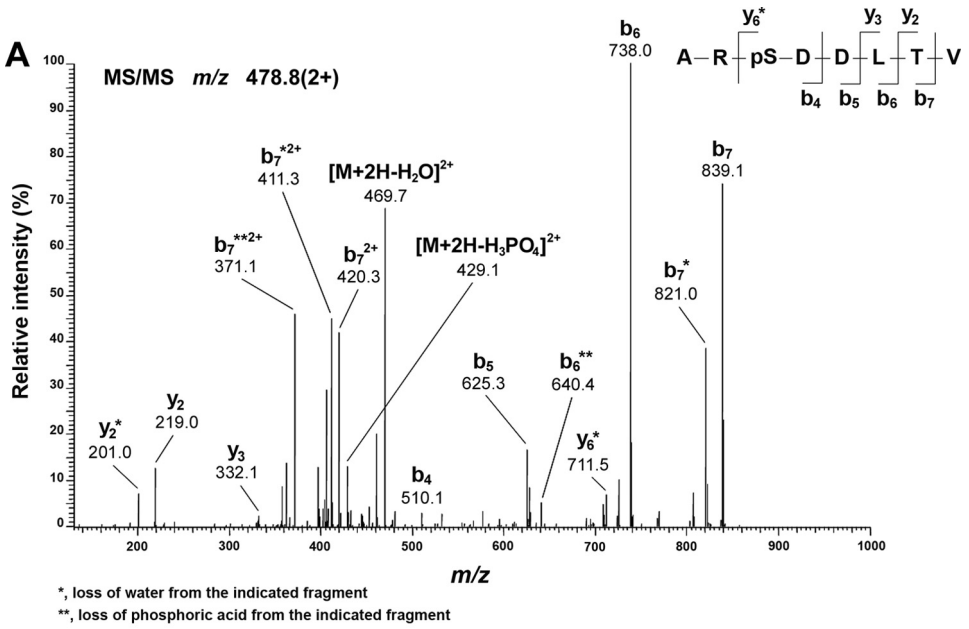

FIGURE 1. **Amino acid residue Ser-395 of Cx50 is phosphorylated in the lens.** Cx50 derived from embryonic chick lenses was purified by immunoprecipitation and digested with trypsin before being subjected to LC-MS/MS. *A*, representative MS/MS spectrum. Assignment of the peptide ARpSDDLTV (Ser(P)-395) is shown. The doubly charged precursor ion, *m/z* 478.8, was fragmented to produce the spectrum. The observed b-fragment (N-terminal) and y-fragment (C-terminal) ions allowed unambiguous localization of phosphorylation at Ser-395. *B*, sequence comparison shows that Ser-395 and residues around this site are highly conserved in Cx50 across animal species.

between the doublet bands in mutants Cx50FS(S395A) and Cx50FS(S387A,S395A) appeared slightly wider than Cx50FS and Cx50FS (S387A). This phenomenon could be caused by mild proteolysis, insufficient reduction of disulfide bonds, or some other unknown reasons.

As shown in Fig. 3*A*, PKA was able to phosphorylate Cx50FS, Cx50FS(S395A), and Cx50FS (S387A) *in vitro* by comparison with GST as a negative control. Surprisingly, the S387A,S395A double mutant of Cx50FS was phosphorylated by PKA, although to a lesser extent compared with Cx50FS and the single mutants (Fig. 3*A*). Comparison of results obtained by two-dimensional TLC indicated that one of the spots in the Cx50FS tryptic phosphopeptide profile (*arrow*) was missing at the corresponding position for the Cx50FS(S395A) mutant, supporting the premise that Ser-395 was phosphorylated by PKA *in vitro* (Fig. 3*B*, *panels a* and *b*); similarly, another spot in Cx50FS tryptic phosphopeptide profile (*white arrow*) was not present at the corresponding position for the Cx50FS(S387A) mutant, indicating that Ser-387 could also be phosphorylated by PKA *in vitro* (Fig. 3*B*, *panels a* and *c*). As expected, both spots were missing at the corresponding positions in the profile of the Cx50FS(S387A,S395A) mutant (Fig. 3*B*, *panel d*).

To examine the kinetics of the phosphorylation process, *in vitro* phosphorylation with PKA was performed for different amounts of time: 5, 15, and 30 min. The phosphorylation of GST-tagged Cx50FS, Cx50FS(S395A), Cx50FS(S387A), and Cx50FS(S387A,S395A), by PKA appeared to reach comparable levels after 30 min, but the double mutant showed a lower degree of phosphorylation after 5 and 15 min of PKA pretreatment (Fig. 3*C*).

To determine whether Cx50 is phosphorylated at the same sites by PKA in the lens *in vivo*, ^{32}P labeling of the chick embryonic lens organs and two-dimensional TLC analysis were performed. Determination of the ^{32}P-labeled tryptic phosphopeptide profile of *in vivo* phosphorylation was made using Cx50 immunoprecipitated from lens samples (Fig. 4, *panel b*). The two-dimensional tryptic phosphopeptide map of a mixture of *in vitro* and *in vivo* phosphorylated samples showed that a spot (*black arrow*) from endogenous Cx50 in the lens migrated at the same position as that of GST-tagged Cx50FS (Fig. 4, *panel c*). Based on the *in vitro* PKA phosphorylation results, this spot represents a tryptic phosphopeptide containing phosphorylated Ser-395 (Fig. 4, *panel a*). The phosphorylation of Cx50 in the lens *in vivo* was further confirmed by pretreating lens organs with the PKA activator 8-Br-cAMP. As shown in Fig. 4 (*panels d* and *e*), this pretreatment increased the phosphorylation level of the tryptic peptide containing Ser-395 by comparing the intensity of the spot for Ser-395 with that of all spots (Fig. 4, *bar plot*). In the two-dimensional tryptic phosphopeptide map of endogenous Cx50 in the lens, there was a very faint

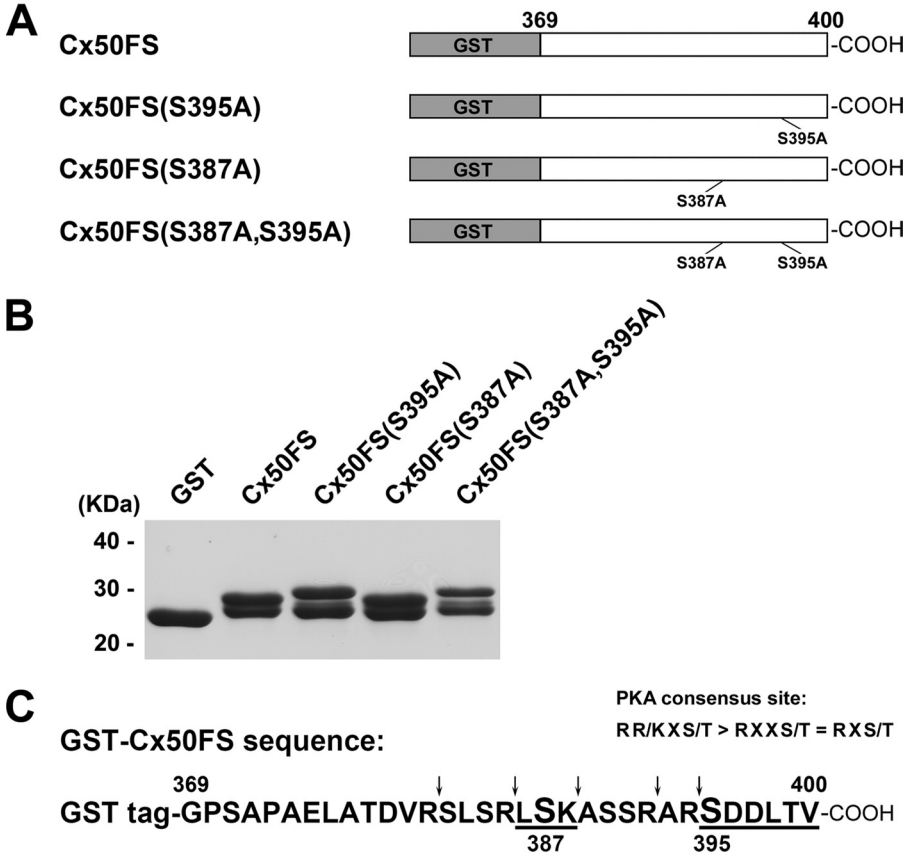

FIGURE 2. **Phosphorylation of GST-tagged Cx50 C terminus fusion proteins and its mutants *in vitro* by PKA.** *A*, schematic representation of GST-tagged Cx50 C terminus fusion proteins and its mutants GST-Cx50FS(S395A, GST-Cx50FS(S387A), and GST-Cx50FS(S387A,S395A). cDNA fragments encoding a short C-terminal tail (*FS*, residues 369–400) of Cx50 were subcloned into GST-tagged expression vector pGEX-2T. Site-directed mutagenesis of serine to alanine was performed by a PCR-based mutagenesis method. *B*, GST-Cx50FS(S395A), GST-Cx50FS(S387A), and GST-Cx50FS(S387A,S395A) were purified and resolved by SDS-PAGE with Coomassie Blue staining. *C*, amino acid residues 369–400 of Cx50 in the GST fusion protein and predicted tryptic cleavage sites are indicated (*arrows*). Both Ser-395 and Ser-387 are located within a PKA consensus site (R(R/K)*X*(S/T) > R*XX*(S/T) = R*X*(S/T)). Their corresponding predicted tryptic peptides are *underlined*.

spot that migrated at a similar position as the tryptic phosphopeptide containing phosphorylated Ser-387, indicating that Ser-387 of Cx50 is not phosphorylated to a major extent under *in vivo* conditions. Taken together, these results support the conclusion that lens Cx50 is phosphorylated at Ser-395 by PKA in the lens *in vivo*.

Phosphorylation of Ser-395 by PKA Increases Cx50 Gap Junction Dye Coupling—To determine whether Ser-395 phosphorylation has any effect on the function of Cx50 gap junctions, CEF cells expressing exogenous Cx50, Cx50(S395A), or Cx50(S387A,S395A) mutants were pretreated with the PKA activator 8-Br-cAMP or forskolin, and gap junction coupling was evaluated by scrape loading dye transfer assay. Similar to wild-type Cx50, Cx50(S395A), and Cx50(S387A,S395A) mutants were able to form functional gap junctions (Fig. 5*A*). In the presence of forskolin or 8-Br-cAMP, gap junction coupling mediated by wild-type Cx50 was increased, but this increase was significantly attenuated in the Cx50(S395A) or Cx50(S387A,S395A) mutants. This result clearly supports the idea that the increased gap junction permeability induced by PKA is at least partially mediated through phosphorylation at Ser-395 of Cx50. Pretreatment by PKA had minimal effect, however, on the expression level of Cx50 protein (Fig. 5*B*), indicating that the enhanced gap junction coupling by PKA was not caused by an increase in the quantity of Cx50.

Both Cx50 and Cx43-mediated Intercellular Communications Were Increased in the Presence of PKA Activators—The effect of PKA on Cx50 gap junctions was also tested in lens primary cultures. Scrape loading dye transfer results showed that both forskolin and 8-Br-cAMP dramatically increased gap junction coupling in lens primary cultures, whereas a specific PKA inhibitor PKI, abolished the increase induced by PKA activators (Fig. 6*A*). Cx50 and Cx43 are the two major connexins expressed in monolayer lens primary cells. To determine the effect of PKA on Cx43 gap junctions, scrape loading dye transfer was performed in connexin-deficient CEF cells expressing exogenous-only Cx50 and/or Cx43. Treatment with 8-Br-cAMP greatly increased Cx50, Cx43, and Cx50/Cx43-mediated intercellular dye coupling (Fig. 6*B*). Together, these results suggest that PKA enhances gap junction communication mediated by both Cx50 and Cx43.

Ser-395 Phosphorylation by PKA Increases Cx50 Hemichannel Activity—Previous studies have shown that Cx50 forms in CEF cells functional hemichannels that are highly responsive to mechanical stimulation (17). A dye uptake analysis was used to determine the effect of Ser-395 phosphorylation by PKA on

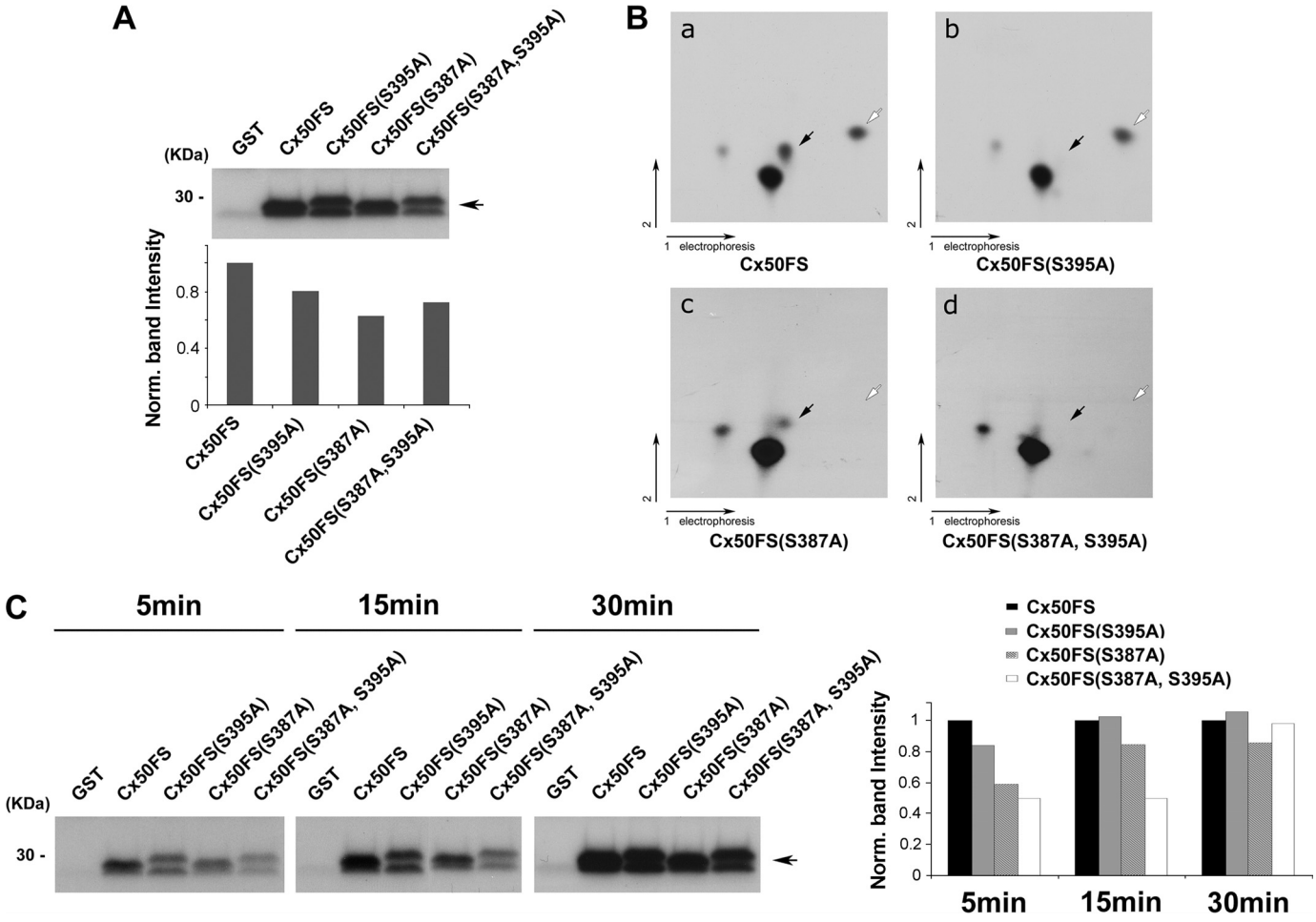

FIGURE 3. **Ser-395 and Ser-387 of Cx50 are phosphorylated by PKA *in vitro*.** *A*, an autoradiogram showing *in vitro* PKA phosphorylation of GST-tagged Cx50 C terminus fusion proteins. Purified GST-Cx50FS, GST-Cx50FS(S395A), GST-Cx50FS(S387A), and GST-Cx50FS(S387A,S395A) were *in vitro* phosphorylated by PKA. GST protein was used as a negative control. Band intensities from Western blots were quantified using densitometry (National Institutes of Health Image J) (*lower panel*). *B*, two-dimensional tryptic phosphopeptide mapping of GST-tagged Cx50 C terminus fusion proteins, Cx50FS (*panel a*), Cx50FS(S395A) (*panel b*), Cx50FS(S387A) (*panel c*), and Cx50(S387A,S395A) (*panel d*). ^{32}P-Labeled GST-tagged Cx50 C terminus fusion proteins were separated by 10% SDS-PAGE, excised, and digested with TPCK-trypsin. The tryptic peptides were applied to two-dimensional TLC at pH 1.9 and then autoradiographed. The *black arrows* indicate the tryptic phosphopeptides containing Ser-395, and the *white arrows* indicate the tryptic phosphopeptides containing Ser-387. *C*, an autoradiogram showing time course analysis of *in vitro* PKA phosphorylation. Purified GST-Cx50FS, GST-Cx50FS(S395A), GST-Cx50FS(S387A), and GST-Cx50FS(S387A,S395A) were *in vitro* phosphorylated by PKA for 5, 15, and 30 min. GST protein was used as a control. Band intensities from Western blots were quantified (*right panel*).

Cx50 hemichannel function. There was minimal dye uptake in CEF cells in the absence of extracellular Ca^{2+} without mechanical stimulation (data not shown). However, when mechanical stimulation was applied by dropping Ca^{2+}-free MEM from a pipette, a comparable increase of dye uptake, as expected from opening hemichannels, was observed in CEF cells that expressed Cx50, Cx50(S395A), or Cx50(S387A,S395A) mutants (Fig. 7). Pretreatment with forskolin significantly increased the hemichannel activities of wild-type Cx50, but this increase was significantly attenuated in cells expressing Cx50(S395A) or Cx50(S387A,S395A) mutant. These results suggest that Ser-395 phosphorylation by PKA also increases Cx50 hemichannel opening.

Ser-395 Phosphorylation by PKA Has Little Effect on the Cell Surface Expression and Gap Junctional Plaque Formation of Cx50—To explore whether the increased channel activities by PKA are due to an increase of Cx50 on the cell surface induced by Ser-395 phosphorylation, cell surface biotinylation was performed. No significant difference in the cell surface expression of Cx50, Cx50(S395A), and Cx50(S387A,S395A) mutants in the absence or presence of forskolin (Fig. 8*A*) was observed. A parallel control assay was conducted with the intracellular protein β-actin, and minimal biotinylation was detected (Fig. 8*A*). The data show that Ser-395 phosphorylation by PKA has little effect on the cell surface expression of Cx50. Because connexins making up gap junctions are normally located within detergent-resistant protein plaques and are therefore less accessible to surface biotinylation than those within hemichannels, we determined the level of Cx50 in junctional plaques using the Triton X-100 extraction approach as previously reported (21) (Fig. 8*B*). The treatment with PKA activators had no effect on the amount of Cx50 in detergent-resistant fractions. Immunofluorescence images also showed similar levels of Cx50 in junctional plaques of PKA activator-treated cells as compared with nontreated controls (Fig. 8*C*). These data suggest that PKA activation does not promote the formation of gap junctional plaques. Together, our findings suggest that the increases in gap junction and

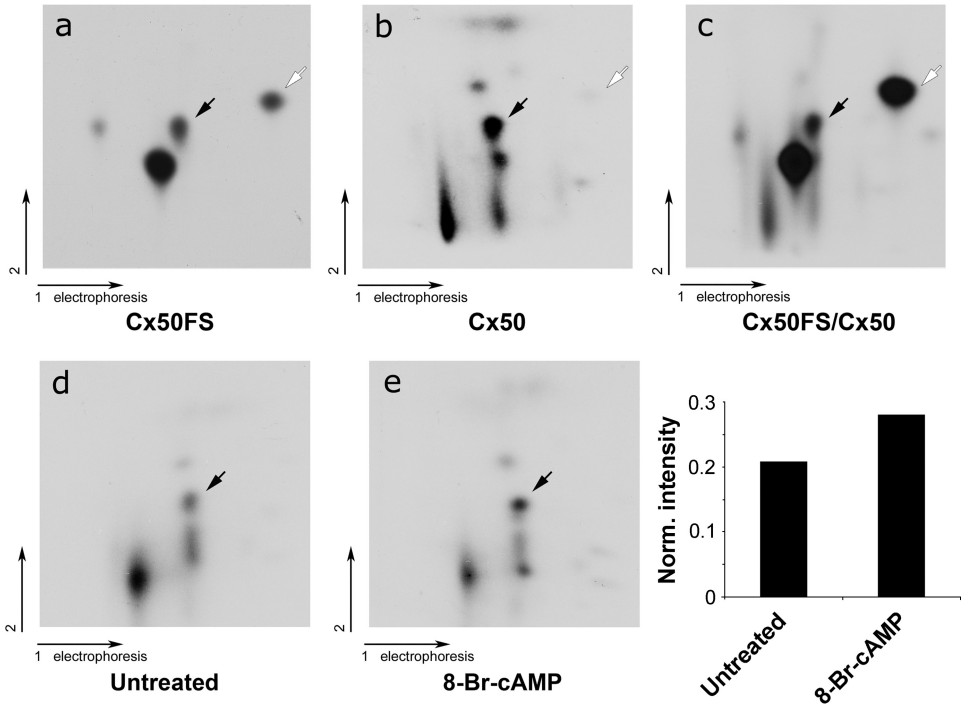

FIGURE 4. **Ser-395 of Cx50 was phosphorylated by PKA in the lens *in vivo*.** Comparison of two-dimensional tryptic phosphopeptide profiles between *in vitro* phosphorylation of GST-Cx50FS by PKA and *in vivo* full-length Cx50. ^{32}P-Labeled phosphorylated Cx50 and GST-Cx50FS were separated by SDS-PAGE, excised, and digested with TPCK-trypsin. The tryptic peptides from phosphorylated Cx50 (*panel a*), GST-Cx50FS (*panel b*), or mixture of both (*panel c*) were applied to two-dimensional TLC at pH 1.9. Tryptic phosphopeptides of full-length Cx50 immunoprecipitated from lenses were pretreated (*panel e*) or untreated (*panel d*) with 1 mM 8-Br-cAMP. The *black arrows* indicate the tryptic phosphopeptides containing Ser-395 phosphorylation, and the *open arrows* indicate the tryptic phosphopeptides containing Ser-387 phosphorylation. Intensities of the dots on *panels d* and *e* were measured using densitometry, and the intensity ratio of the spot representing Ser-395 *versus* all spots is presented (*bottom right panel*).

hemichannel activities induced by PKA phosphorylation at Ser-395 are not caused by an increased level of total Cx50 protein, Cx50 on the cell surface, or gap junction plaque formation but most likely are caused through the regulation of conductivity or gating properties of Cx50 channels.

PKA Activation Increases the Frequency of More Conductive Channels—Increases in gap junction mediated dye coupling could result from increased numbers of channels, which seems precluded by the above data, increased permeability of the individual channels, and/or increased open probability of the channels. To evaluate possible increases in permeability of the individual channels, we recorded the channel activity of Cx50 and Cx50(S395A) expressed in Rin cells treated or not with 8-Br-cAMP. Channel behavior and the corresponding all points histograms (Fig. 9 and supplemental Fig. S2) revealed for both wild-type and mutant proteins several commonly occupied open states, including ~35, 65, and 200 pS and a relatively rarely occupied open state of 250 pS. These same open states were also observed in 8-Br-cAMP-treated cells. It is noteworthy that channels opening from base line (zero current level) were extremely rare, with channels open to apparently long-lasting residual state(s) nearly always revealed when transjunctional voltage was returned to zero (supplemental Fig. S2).

Transitions between these channel open states were measured for Cx50-expressing cells, in both the absence and presence of PKA activation. Given the conductances of the open states observed for Cx50 channels, transitions with the following conductances were expected: 35 and 65 pS (between closed and residual states), 135–165 pS (between residual and 200 pS states), and 200 pS (between closed and 200 pS states). The best fit (R^2 = 0.98) of the channel transition amplitude histogram (Fig. 10*A*, *top panel*) revealed four peaks corresponding to 59, 145, 202, and 242 pS, with 74% of observed transitions in the peak corresponding to 145 pS. These data indicate that in the absence of PKA activation, Cx50 channels transition most frequently between the ~65 pS residual and ~200 pS open states, although transitions between the closed state and each of open states were also evident. In the presence of PKA activation, the best fit (R^2 = 0.95) of the amplitude histogram (Fig. 10*A*, *bottom panel*) revealed peaks at 58, 102, 186, and 251 pS, with 84% of transitions in the peak corresponding to 186 pS. The principal difference in behavior of the Cx50 channel induced by PKA activation was thus an increased prevalence of transitions between the closed and ~200 pS open states, with a corresponding decrease in transitions between the ~65 pS residual and ~200 pS open states. These results suggest that the ~200 pS conductance state of Cx50 might underlie the PKA-induced increase in dye coupling.

The channel transition amplitude histogram for Cx50(S395A) channels in untreated cells (Fig. 10*B*, *top panel*) also revealed four peaks with conductances corresponding to 72, 135, 193, and 284 pS. Interestingly, for the mutant channel, transitions between the closed and ~200 pS states predominated in the untreated cells, with 84% of the observed transitions (R^2 = 0.97). Thus, the behavior of the mutant channel did not mimic the behavior of the untreated wild-type channel but rather resembled that of the treated wild-type channel (supplemental Fig. S3, *A versus B*). Despite the similarity to the treated wild-

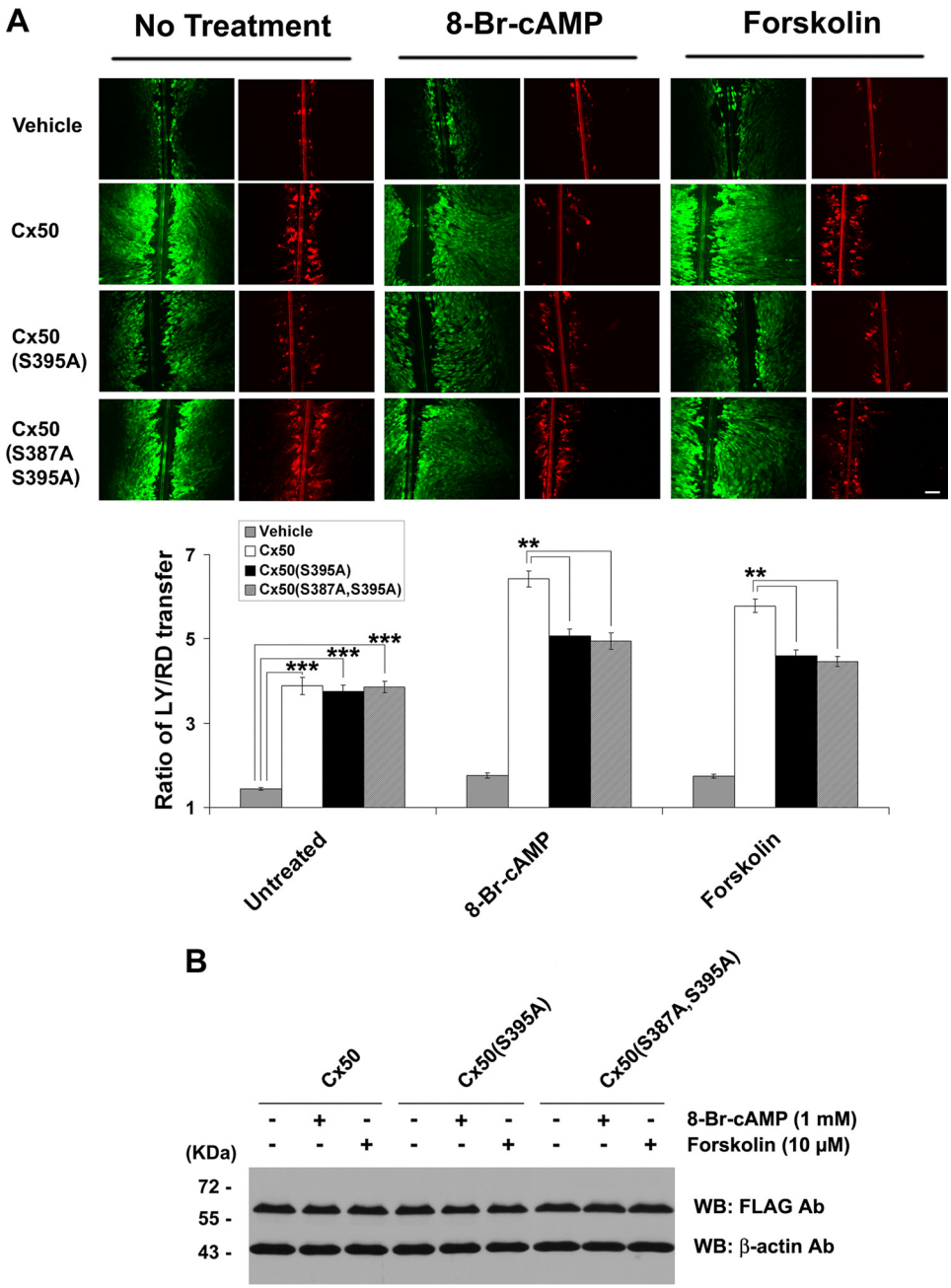

FIGURE 5. **Phosphorylation of Ser-395 by PKA increases Cx50 gap junction coupling but has no effect on Cx50 protein level.** *A*, CEF cells expressing exogenous Cx50, Cx50(S395A), or Cx50(S387A,S395A) mutant in the absence or presence of PKA activator: 8-Br-cAMP (1 mM) or forskolin (10 μM) for 2 h before scrape loading dye transfer assay using LY (*green*) as a probe for gap junctional coupling and RD (*red*) as a tracer for originally dye-loaded cells (*upper panel*). *Bar*, 50 μm. Both forskolin and 8-Br-cAMP significantly increased Cx50 gap junction coupling, and this increase was significantly reduced in cells expressing Ser-395 mutant (*lower panel*; $n = 6$). *B*, CEF cells expressing Cx50 or the S395A mutant were detected by Western blotting (*WB*) using anti-FLAG antibody (1:1000 dilution) after being treated with 8-Br-cAMP (1 mM) or forskolin (10 μM) for 2 h. The membranes were stripped and reblotted with monoclonal antibody against the control protein, β-actin.

type channel, PKA activation of Cx50(S395A)-expressing cells altered the behavior of the mutant channels (Fig. 10*B*, *bottom panel*). The frequencies of the 72, 135, and 250 pS transitions were increased by PKA activation, whereas the frequency of ~200 pS transitions decreased ($R^2 = 0.94$). Given the initial differences between the untreated wild-type and mutant junctions, the most remarkable effect of PKA activation on the Cx50(S395A) channel was an increase in the frequency of largest ~250 pS transitions.

Open probability ($P_o = t_o/(t_o + t_c)$, where t_o is open time, and t_c is closed time) is not readily measured for gap junction channels, because multiple channels are nearly always present in gap junctions. Nevertheless, an increase in open probability resulting from an increase in open time can often be detected (23–26). To determine whether such an increase occurred for either Cx50 or Cx50(S395A) as a result of PKA activation, we measured open time duration. For both wild-type and mutant channels, open time (supplemental Fig. S4; for events of all ampli-

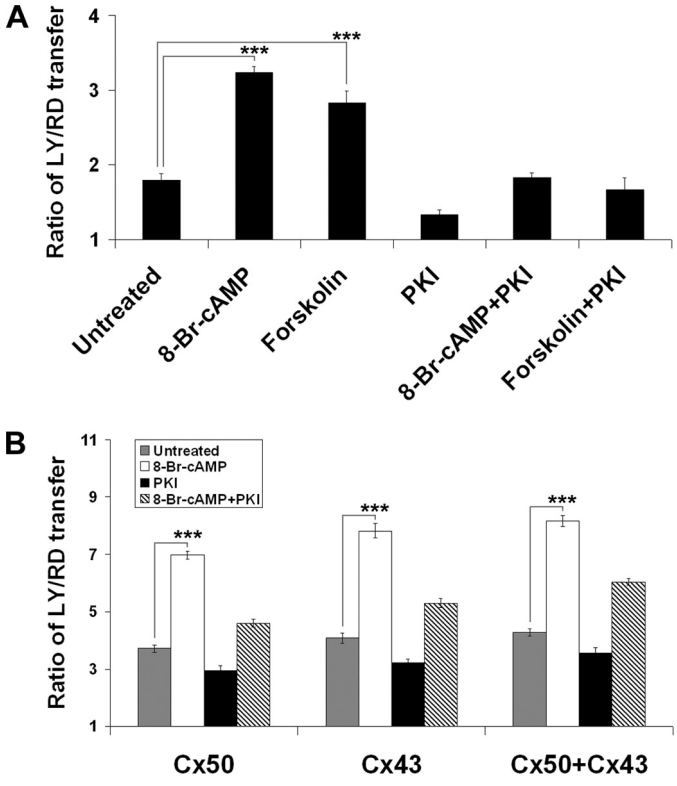

FIGURE 6. **PKA activators increase Cx50 and Cx43-mediated intercellular communications.** *A*, lens primary cultures were treated or not with 8-Br-cAMP (1 mM) or forskolin (10 μM) and/or PKI (0.4 μM) for 2 h before scrape loading dye transfer assay. Both forskolin and 8-Br-cAMP dramatically increased Cx50/Cx43 gap junction coupling in lens primary cultures ($n = 6$). *B*, CEF cells expressing exogenous Cx50, Cx43, or both Cx50 and Cx43 were treated or not with 8-Br-cAMP (1 mM) and/or PKI (0.4 μM) for 2 h before scrape loading dye transfer assay. 8-Br-cAMP greatly increased Cx50, Cx43, and Cx50/Cx43-mediated intercellular communications ($n = 6$).

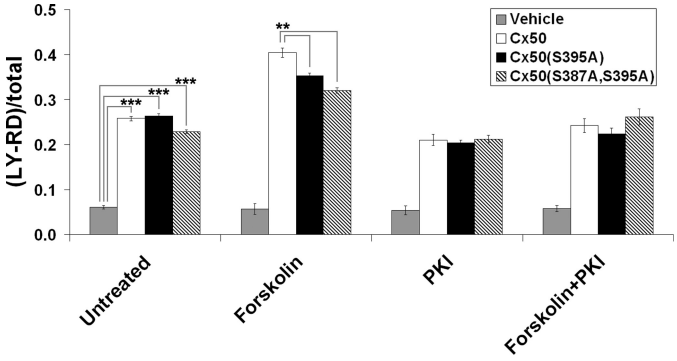

FIGURE 7. **Cx50 hemichannel activities were increased by Ser-395 phosphorylation.** CEF cells infected with recombinant retroviruses containing Cx50, Cx50(S395A), Cx50(S387A,S395A) mutant, or RCAS(A) vehicle control were cultured at low cell density with no physical contact. The numbers of cells with LY/RD dye uptake with or without mechanical stimulation by dropping the medium were counted and quantified. Dye uptake was presented as a percentage of fluorescent cells divided by the total number of cells ($n = 3$).

tudes irrespective of amplitude) decreased slightly with PKA activation (WT, from 1.03 to 0.83 s; S395A, from 1.66 to 1.07 s). To discern whether the open time of ~200 pS events (transitions from closed to this open state) accounted for this decrease in overall open time, the open times of events corresponding to this and the residual state were examined (supplemental Figs. S5 and S6). No obvious changes in open time duration of the Cx50 or Cx50(S395A) ~200 pS channel occurred.

DISCUSSION

Here, we identified for the first time an important *in vivo* phosphorylation site in the C terminus of lens Cx50. Overall, our results indicated that Ser-395 of Cx50 is phosphorylated by PKA in the lens and that this phosphorylation enhanced both Cx50 gap junction coupling and hemichannel activities. In contrast to PKA-induced Cx43 phosphorylation, this enhancement is not likely through an increase of total Cx50 expression level, Cx50 on the cell surface, or gap junction plaque formation but probably an effect on channel gating.

Mass spectrometry is an invaluable tool to locate phosphorylation sites on proteins. By using tandem mass spectrometry, we showed that Cx50 is *in vivo* phosphorylated at Ser-395 in the embryonic chick lens, further confirming a recent report that the corresponding serine residue of bovine Cx50 is phosphorylated in the lens *in vivo* (14). Our comparative sequence analysis shows that the Ser-395 in the C-terminal end of Cx50 is highly conserved across various species.

Both Ser-395 and Ser-387 of Cx50 are located within PKA consensus phosphorylation sites. PKA is a cAMP-dependent enzyme implicated in a wide range of cellular processes. Multiple studies have shown that cAMP-enhanced Cx43 gap junction coupling appears to be mediated by PKA either by direct phosphorylation of Ser-364 or by activating another kinase that actually phosphorylates Cx43 at Ser-364 (27–29). Phosphorylation of this site is critical for cAMP-enhanced Cx43 gap junction assembly, even though Cx43 is a relatively poor substrate for PKA compared with PKC or MAPK (30, 31). *In vitro* phosphorylation and mutagenesis analyses showed that Cx35, a major component of electrical synapses in the central nervous system, can also be directly phosphorylated by PKA. Moreover, PKA regulates Cx35 coupling in a complex manner that requires two phosphorylation sites as well as the C terminus end acting as a "switch" that determines whether phosphorylation will inhibit or enhance coupling (32, 33). In zebrafish retina, the magnitude of photoreceptor coupling is controlled by the dynamic phosphorylation/dephosphorylation of Cx35 (34). Phosphorylation of Cx36 (the mammalian homologue of Cx35) by PKA leads to a down-regulation of gap junction permeability, which acts as a molecular switch in modulating Cx36 coupling and light adaptation in the mouse retina (35). Although PKA is also likely involved in the phosphorylation of chicken Cx56, treatment with PKA activators did not induce substantial changes in Cx56 tryptic phosphopeptide pattern (12).

Comparison of two-dimensional tryptic phosphopeptide profiles indicated that both Ser-395 and Ser-387 of Cx50 were phosphorylated by PKA *in vitro*. Surprisingly, Cx50(S387A,S395A) mutant was still phosphorylated by PKA *in vitro*. These data implicate the possibility of additional PKA phosphorylation site(s). Cx50FS contains a total of seven serine residues and two threonine residues (including Ser-395 and Ser-387). Previous studies have shown that chicken Cx50 is phosphorylated only on serine residues (7). It is then possible that, *in vitro*, additional serine residue(s) besides Ser-395 and Ser-387 are phosphorylated by PKA. For instance, overphosphorylation may occur because of excessive levels of kinase and

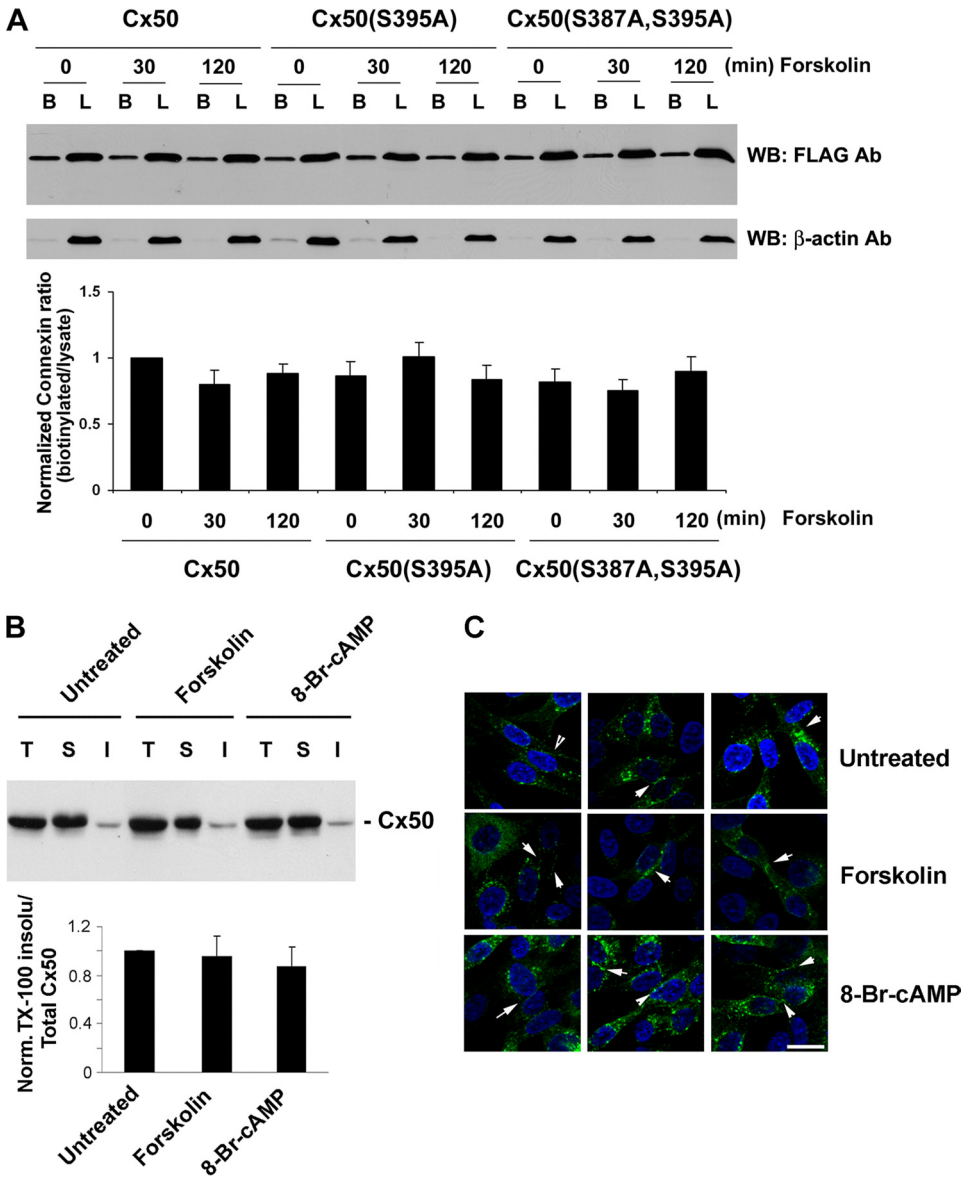

FIGURE 8. **Ser-395 phosphorylation has no effect on the cell surface expression and junction plaque formation of Cx50.** *A*, 6 days after infection with recombinant retroviruses containing Cx50, Cx50(S395A), or Cx50(S387A,S395A) mutant, CEF cells were pretreated or not with PKA activator forskolin (10 μM) for 0, 30, or 120 min before applying Sulfo-NHS-LC-Biotin. Equal volumes of total protein of cell lysates were applied to neutravidin-conjugated beads. The biotinylated proteins were eluted, and proportional amounts of preloaded cell lysates (*lanes L*) and biotinylated proteins bound to neutravidin beads (*lanes B*) were detected by Western blotting (*WB*) using anti-FLAG antibody (1:1000 dilution). The membranes were stripped and reblotted with monoclonal antibody against the control protein, β-actin. The relative ratio of biotinylated connexin to total connexin was quantified by using densitometric measurements of the band intensity (*lower panel*, $n = 3$). *B*, CEF cells expressing exogenous Cx50 were treated or not with PKA activator: 8-Br-cAMP (1 mM) or forskolin (10 μM) for 2 h. Isolated membrane samples were treated with 1% Triton X-100. The detergent-soluble (*lanes S*) and -insoluble (*lanes I*) fractions were separated by centrifugation and analyzed along with total (*lanes T*) membrane samples by Western blotting using anti-Cx50 antibody (1:500 dilution). The relative ratio of Triton X-100-insoluble to total Cx50 was quantified by using densitometric measurements of the band intensity (*lower panel*, $n = 3$). *C*, CEF cells were immunolabeled with anti-Cx43 antibody followed by FITC-conjugated anti-rabbit IgG (*green*). The nuclei were stained with DAPI (*blue*). *Bar*, 15 μm.

substrates. We conducted *in vitro* phosphorylation with a shorter reaction time and found that Cx50FS and its mutants were phosphorylated by PKA in a time-dependent manner, so that during brief treatments, reduced phosphorylation intensity was seen. Also possible is that the protein conformation and accessibility to the phosphorylation sites in the fusion proteins could be different from those in the complete Cx50 molecule. However, tryptic phosphopeptides from Cx50FS and Cx50 yielded a coincidental pattern when ran together. In contrast to the *in vitro* data, the two-dimensional tryptic phosphopeptide mass spectrometry analyses of endogenous Cx50 showed that Ser-395 was the major site phosphorylated by PKA in the lens *in vivo*.

To explore the functional importance of phosphorylation at Ser-395, a retroviral expression approach was used for the efficient introduction of exogenous proteins into connexin-deficient CEF cells and primary lens cultures. We showed that, similar to wild-type Cx50, both Cx50(S395A) and Cx50(S387A,S395A) were able to form functional gap junctions. Because CEF cells in culture usually have a lower phos-

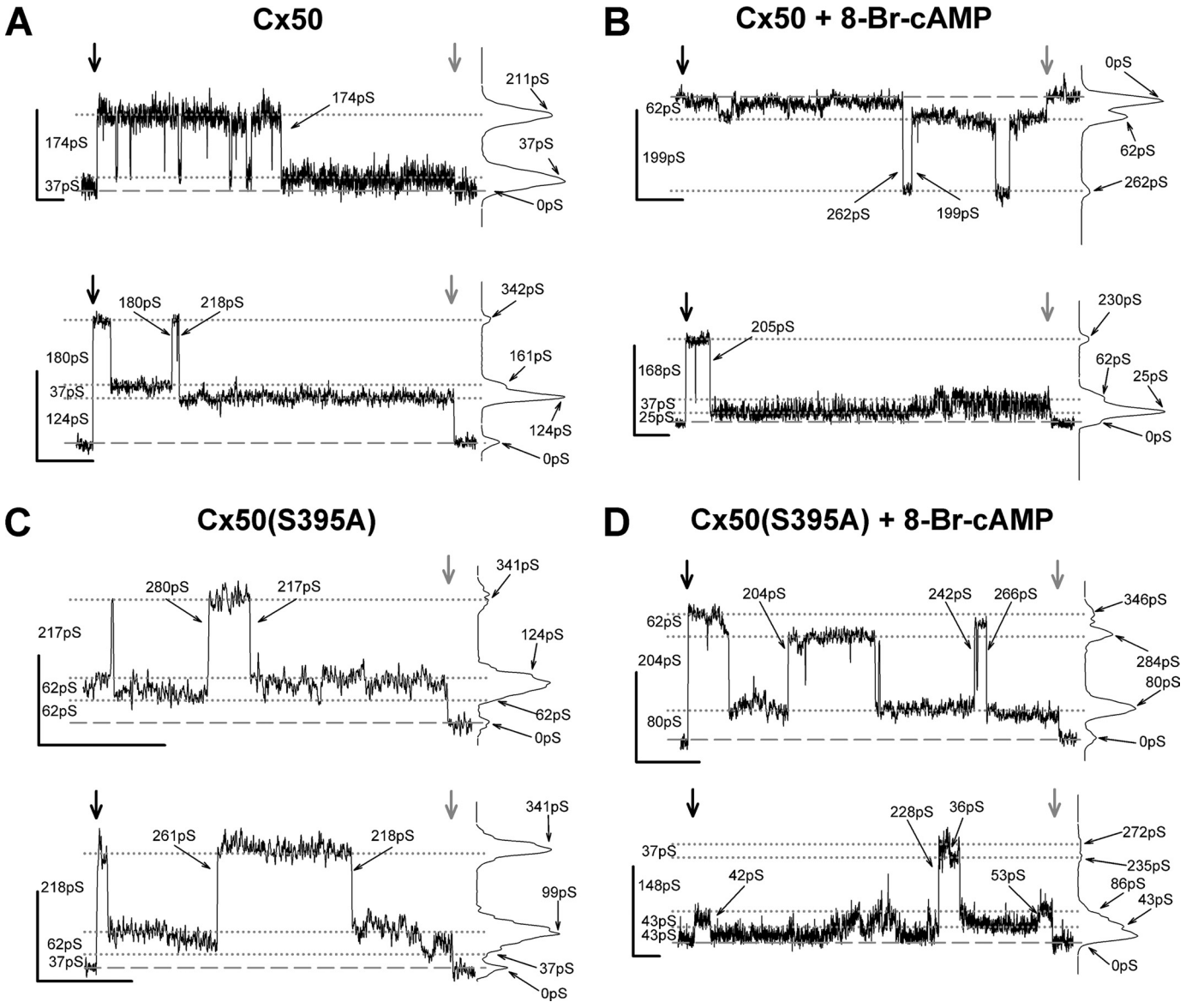

FIGURE 9. **Open state conductances of Cx50 and Cx50(S395A) comprised channels are comparable.** Primary records and associated all points histograms from Cx50 (*A* and *B*) and Cx50(S395A) mutant (*C* and *D*) gap junctions illustrate channel activity and event amplitudes in the absence (*A* and *C*) and in the presence (*B* and *D*) of 8-Br-cAMP. Recordings were screened for sections with only one large amplitude channel event evident, and amplitudes of all current levels were measured. Traces (two examples for each group) show some of the amplitudes encountered and the variability of channel behavior. All points histograms are displayed to the *right* of each trace. *Broad vertical arrows* mark the start (*black*) and end (*gray*) of the transjunctional voltage pulse, except for upper trace in *C*, where the start of a longer pulse is not shown. *Black lines* mark the base line (*dashed*) and several (*dotted*) current levels; conductance values on the *left* of each trace indicate the conductance differences between these successive levels. The *small arrows* and values on the histograms indicate the cumulative conductance values from base line; *small arrows* and values on the traces show the conductances of indicated transitions. Calibration for all traces: $y = 10$ pA; $x = 2$ s. The conductance steps were calculated as $\gamma_j = I_j/V_j$, where $V_j = \pm 40$ mV.

phorylation level compared with the lens cells *in vivo*, differences in coupling between wild-type and mutant forms of Cx50 might have been overlooked in CEF cells in the absence of PKA activation. The two PKA activators used (forskolin and 8-Br-cAMP) enhanced gap junction dye coupling by Cx50, and this increase was significantly and comparably attenuated in cells expressing the single S395A or double S387A,S395A mutant of Cx50. The lack of differential response between the double and single S395A mutants suggests that Ser-387 was unlikely to be functionally involved in PKA-dependent regulation of Cx50 gap junctions. Because PKA activators increase dye coupling and dye uptake in the double mutant (S387A,S395A)-expressing cells (although to a lesser degree that in cells expressing wild-type Cx50), we cannot completely exclude the possibility of minor phosphorylation at other potential PKA site(s) or phosphorylation by other kinase(s) activated by PKA. Alternatively, PKA activation may enhance Cx50 channel function by triggering unidentified mechanism(s).

The enhancement of Cx43-mediated gap junction intercellular communication by PKA is mediated by up-regulation of Cx43 trafficking and assembly (2, 5). In contrast, the PKA-induced increased coupling by Cx50 was not likely through the enhancement of total protein expression or the quantity of Cx50 on the cell surface or in gap junctional plaques. Therefore, these increases in dye coupling may reflect changes in channel open probability or unitary per-

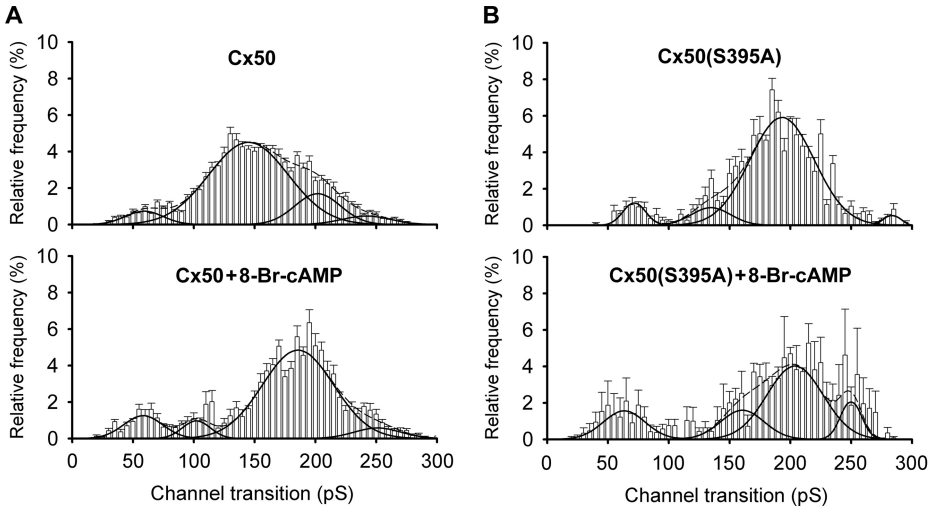

FIGURE 10. **PKA activation affects the behavior of Cx50 (*A*) and Cx50(S395A) mutant (*B*) channels.** Histograms of events in the absence (*top panels*) and in the presence of 8-Br-cAMP (*bottom panels*) revealed for the wild-type protein a large decrease in frequency of transitions between the residual and ~200 pS open state (~145 pS transitions) and a corresponding increase in frequency of transitions between the closed and ~200 pS open state following PKA activation. For the mutant channel, the histogram of untreated channels appears similar to the histogram for treated wild-type channels, with PKA inducing a decrease in frequency of the closed to ~200 pS open state transitions, with increases in frequency of all other transition types. Interval = 5 pS; *black lines* indicate the fit for every peak (*solid lines*) and the sum of all fits (*dashed lines*). Fit parameters for each plot (conductance and percentage of events for each peak and overall quality of fit) were as follows: Cx50 untreated, 59 ± 3 pS (6%), 145 ± 0 pS (fixed width) (74%), 202 ± 8 pS (16%), and 242 ± 30 pS (5%) (R^2 = 0.98; number of experiments, n = 11, number of transitions, n = 2540); Cx50 treated, 58 ± 2 pS (11%), 102 ± 2 pS (6%), 185 ± 2 pS (77%), and 251 ± 9 pS (6%) (R^2 = 0.95; n = 6, n = 889); Cx50(S395A) untreated, 72 ± 1 pS (6%), 135 ± 6 pS (8%), 193 ± 2 pS (84%), and 284 ± 1 pS (2%) (R^2 = 0.97; n = 5, n = 676); and Cx50(S395A) treated, 62 ± 3 pS (16%), 101 ± 16 pS (17%), 204 ± 8 pS (56%), and 250 ± 5 pS (11%) (R^2 = 0.94; n = 3, n = 950).

meability. The "ball-and-chain" model of gap junction channel gating hypothesizes that the C-terminal domain of connexin may act as a gating particle by binding to specific region(s) of the cytoplasmic loop (36, 37) and thereby reversibly (in a pH, voltage or phosphorylation dependent manner) reducing channel permeation. Our single channel records showed channel conductances very similar to those previously published for chick and mammalian forms of Cx50 (23, 38–40). Amplitude histograms of Cx50 channel transitions demonstrated that PKA activation increased the frequency of transitions between the closed and ~200 pS conductance state while reducing the frequency of transitions between the ~65 pS residual and ~200 pS conductance states (Fig. 10) without affecting the open time of the ~200 pS channel. If this PKA-induced change in channel behavior explains the PKA-induced increase in dye coupling, then the ~200 pS conductance state would presumably have higher dye permeability than either the ~65 or ~35 pS residual (and closed) states. In addition, because phosphorylation was associated with increased permeation, the ball-and-chain model of channel function would suggest that the frequency of interaction between the C-terminal and loop domains would be reduced as a consequence of PKA-dependent phosphorylation, thereby allowing the channel to be more fully open.

If phosphorylation at Ser-395 were the unique biochemical event triggering changes in both macroscopic permeability and channel conductance, then one would expect the mutant Cx50(S395A) junctions and channels would be unable to display either effect. As our data show, untreated Cx50(S395A) junctions displayed channel conductance behavior very similar to that of the 8-Br-cAMP-treated Cx50 channels (Fig. 10 and supplemental Fig. S3), with a high frequency of ~200 pS transitions. This indicates that phosphorylation at Ser-395 is unnecessary for such profile of channel conductance behavior. Although unnecessary for increased frequency of ~200 pS transitions, phosphorylation at Ser-395 may nevertheless facilitate or be permissive to adoption of a high permeability configuration by the channel composed of wild-type Cx50. Perhaps phosphorylation at other sites (including C-terminal sites) is necessary for the full response of Cx50 to PKA, so that the absence of Ser-395 in the mutant junctions impairs but does not eliminate, the PKA induced increase in dye coupling while still supporting transitions between the closed and ~200 pS conductance states. The implications of this would be that phosphorylation of the channel proteins can alter the channel dye permeability without altering its conductance (22, 41), which seems plausible given the large number of phosphorylation sites and limited number of conductance states displayed by most gap junction channels.

In addition to forming gap junctions, connexins can also form functional hemichannels in nonjunctional membranes, which play a distinct role in the communication of cells with their extracellular space (42). Hemichannels formed by lens fiber connexins are postulated to be mechano-sensitive and might have a physiological role permitting rapid fluid equilibration under the mechanical stress associated with accommodation (43). We have previously shown that Cx50 hemichannels can be induced to open in response to mechanical stimulation (17). Similar to increased gap junction-mediated dye coupling, hemichannel activity of Cx50 was increased in the presence of a PKA activator, and this increase was significantly attenuated in the S395A mutant. Thus, our findings

indicate that Ser-395 phosphorylation plays a vital role in promoting dye permeation of both Cx50 gap junctions and hemichannels in a manner independent of Cx50 expression or localization.

We showed that PKA activators dramatically increased gap junction dye coupling in lens primary cultures. Cx50 and Cx43 are the two major connexins expressed in lens epithelial cells, with Cx50 playing the major role in dye coupling during early postnatal lens development and Cx43 contributing more at later developmental stages (44). The increase in dye coupling induced by PKA activators in lens primary cultures could be contributed by PKA-mediated phosphorylation of either or both Cx50 and Cx43. We showed that PKA activation increased dye coupling in CEF cells expressing Cx43 individually or together with Cx50. This is consistent with the results of previous studies demonstrating that elevation of intracellular cAMP increased Cx43 phosphorylation and Cx43-mediated intercellular communication (2).

Co-expression of murine Cx50 and Cx43 produced, in frog oocytes, lower electrical coupling than that of either connexin alone and in epithelial cells produced charge selectivity and permeability intermediate to those of the homomeric junctions (45). These observations suggest that the presence of Cx43 influences the regulation of Cx50. Because our goal was to evaluate the role of Ser-395 in junctional regulation, no attempt at dissecting the participation of each connexin in the response to PKA was made in this study. However, we showed that PKA enhances the permeability of Cx50 and Cx43, alone or co-expressed, in lens primary cultures. Moreover, the permeability for Cx50, Cx43, and Cx50+Cx43 junctions seems comparable before and after PKA activation. However, it is interesting to consider how differences in overall coupling will affect cell transjunctional exchange at various regions of the lens, particularly at the junctions between epithelial and fiber cells. Hypothetically, low coupling would tend to preserve voltage differences, such as may exist at heterocellular junctions, and strong voltage differences might favor residually open channels and limit transjunctional exchange to the smallest permeants, but at the same time accelerate the diffusion of the most charged ones along this cell-to-cell electrical gradient. Conversely, increased coupling would tend to decrease the electrical gradient and allow the diffusion of bigger molecules, but this diffusion would be limited by their own chemical gradient, the selectivity of the connexin(s) present, and their specific regulatory signals. The connexins discussed here have diverse selectivity: Cx43 is highly permeable but not very charge selective (22, 46), whereas Cx50 may be cation-selective but less permeable than Cx43 (45). Earlier studies showed that adenylate cyclase activity is predominantly localized in the outer cortical region of the lens (47). Based on the proposed lens microcirculation model (48), this is the region where fluid and metabolic wastes are disposed. Therefore, there is a high demand for cell-cell coupling to accommodate these metabolic needs. Phosphorylation of Cx50 (and possibly Cx43) by cAMP-activated PKA could greatly enhance gap junction communication in this region and facilitate the physiological functions of the lens.

Acknowledgments—We thank Dr. D. L. Paul at the Harvard Medical School for providing the pIRE2-EGFP vector, Drs. L. Zhou and F. Liu at the UTHSCSA for technical assistance for two-dimensional tryptic phosphopeptide mapping analysis, and members of the Jiang laboratory for critical reading of the manuscript. Mass spectrometry analyses were conducted with the assistance of Christopher A. Carroll in the UTHSCSA Institutional Mass Spectrometry Laboratory.

REFERENCES

1. Meşe, G., Richard, G., and White, T. W. (2007) *J. Invest. Dermatol.* **127,** 2516–2524
2. Lampe, P. D., and Lau, A. F. (2004) *Int. J. Biochem. Cell Biol.* **36,** 1171–1186
3. Solan, J. L., and Lampe, P. D. (2009) *Biochem. J.* **419,** 261–272
4. Cruciani, V., and Mikalsen, S. O. (2002) *Biol. Cell.* **94,** 433–443
5. Solan, J. L., and Lampe, P. D. (2005) *Biochim. Biophys. Acta.* **1711,** 154–163
6. Gong, X., Cheng, C., and Xia, C. H. (2007) *J. Membr. Biol.* **218,** 9–12
7. Jiang, J. X., and Goodenough, D. A. (1998) *Eur. J. Biochem.* **255,** 37–44
8. Cheng, H. L., and Louis, C. F. (1999) *Eur. J. Biochem.* **263,** 276–286
9. Cheng, H. L., and Louis, C. F. (2001) *J. Membr. Biol.* **181,** 21–30
10. Yin, X., Jedrzejewski, P. T., and Jiang, J. X. (2000) *J. Biol. Chem.* **275,** 6850–6856
11. Yin, X., Gu, S., and Jiang, J. X. (2001) *J. Biol. Chem.* **276,** 34567–34572
12. Berthoud, V. M., Beyer, E. C., Kurata, W. E., Lau, A. F., and Lampe, P. D. (1997) *Eur. J. Biochem.* **244,** 89–97
13. Shearer, D., Ens, W., Standing, K., and Valdimarsson, G. (2008) *Invest. Ophthalmol. Vis. Sci.* **49,** 1553–1562
14. Wang, Z., and Schey, K. L. (2009) *Exp. Eye. Res.* **89,** 898–904
15. Jiang, J. X., White, T. W., Goodenough, D. A., and Paul, D. L. (1994) *Mol. Biol. Cell.* **5,** 363–373
16. Jiang, J. X. (2001) *Methods Mol. Biol.* **154,** 159–174
17. Banks, E. A., Toloue, M. M., Shi, Q., Zhou, Z. J., Liu, J., Nicholson, B. J., and Jiang, J. X. (2009) *J. Cell Sci.* **122,** 378–388
18. el-Fouly, M. H., Trosko, J. E., and Chang, C. C. (1987) *Exp. Cell Res.* **168,** 422–430
19. Cherian, P. P., Siller-Jackson, A. J., Gu, S., Wang, X., Bonewald, L. F., Sprague, E., and Jiang, J. X. (2005) *Mol. Biol. Cell.* **16,** 3100–3106
20. Daniels, G. M., and Amara, S. G. (1998) *Methods Enzymol.* **296,** 307–318
21. Musil, L. S., and Goodenough, D. A. (1991) *J. Cell Biol.* **115,** 1357–1374
22. Ek-Vitorin, J. F., King, T. J., Heyman, N. S., Lampe, P. D., and Burt, J. M. (2006) *Circ. Res.* **98,** 1498–1505
23. Srinivas, M., Costa, M., Gao, Y., Fort, A., Fishman, G. I., and Spray, D. C. (1999) *J. Physiol.* **517,** 673–689
24. Moreno, A. P., Chanson, M., Elenes, S., Anumonwo, J., Scerri, I., Gu, H., Taffet, S. M., and Delmar, M. (2002) *Circ. Res.* **90,** 450–457
25. Xu, X., Berthoud, V. M., Beyer, E. C., and Ebihara, L. (2002) *J. Membr. Biol.* **186,** 101–112
26. Shibayama, J., Gutiérrez, C., González, D., Kieken, F., Seki, A., Carrión, J. R., Sorgen, P. L., Taffet, S. M., Barrio, L. C., and Delmar, M. (2006) *Biophys. J.* **91,** 4054–4063
27. Burghardt, R. C., Barhoumi, R., Sewall, T. C., and Bowen, J. A. (1995) *J. Membr. Biol.* **148,** 243–253
28. Atkinson, M. M., Lampe, P. D., Lin, H. H., Kollander, R., Li, X. R., and Kiang, D. T. (1995) *J. Cell Sci.* **108,** 3079–3090
29. Paulson, A. F., Lampe, P. D., Meyer, R. A., TenBroek, E., Atkinson, M. M., Walseth, T. F., and Johnson, R. G. (2000) *J. Cell Sci.* **113,** 3037–3049
30. TenBroek, E. M., Lampe, P. D., Solan, J. L., Reynhout, J. K., and Johnson, R. G. (2001) *J. Cell Biol.* **155,** 1307–1318
31. Shah, M. M., Martinez, A. M., and Fletcher, W. H. (2002) *Mol. Cell Biochem.* **238,** 57–68
32. Mitropoulou, G., and Bruzzone, R. (2003) *J. Neurosci. Res.* **72,** 147–157
33. Ouyang, X., Winbow, V. M., Patel, L. S., Burr, G. S., Mitchell, C. K., and O'Brien, J. (2005) *Brain Res. Mol. Brain Res.* **135,** 1–11

34. Li, H., Chuang, A. Z., and O'Brien, J. (2009) *J. Neurosci.* **29,** 15178–15186
35. Urschel, S., Höher, T., Schubert, T., Alev, C., Söhl, G., Wörsdörfer, P., Asahara, T., Dermietzel, R., Weiler, R., and Willecke, K. (2006) *J. Biol. Chem.* **281,** 33163–33171
36. Stergiopoulos, K., Alvarado, J. L.,Mastroianni, M., Ek-Vitorin, J. F., Taffet, S. M., and Delmar, M. (1999) *Circ. Res.* **84,** 1144–1155
37. Anumonwo, J. M., Taffet, S. M., Gu, H., Chanson, M., Moreno, A. P., and Delmar, M. (2001) *Circ. Res.* **88,** 666–673
38. Ebihara, L., Xu, X., Oberti, C., Beyer, E. C., and Berthoud, V. M. (1999) *Biophys. J.* **76,** 198–206
39. Tong, J. J., and Ebihara, L. (2006) *Biophys. J.* **91,** 2142–2154
40. Donaldson, P. J., Dong, Y., Roos, M., Green, C., Goodenough, D. A., and Kistler, J. (1995) *Am. J. Physiol.* **269,** C590–C600
41. Heyman, N. S., and Burt, J. M. (2008) *Biophys. J.* **94,** 840–854
42. Goodenough, D. A., and Paul, D. L. (2003) *Nat. Rev. Mol. Cell. Biol.* **4,** 285–294
43. Bao, L., Sachs, F., and Dahl, G. (2004) *Am. J. Physiol.* **287,** C1389–C1395
44. White, T. W., Gao, Y., Li, L., Sellitto, C., and Srinivas, M. (2007) *Invest. Ophthal. Vis. Sci.* **48,** 5630–5637
45. DeRosa, A. M., Meşe, G., Li, L., Sellitto, C., Brink, P. R., Gong, X., and White, T. W. (2009) *Exp. Cell Res.* **315,** 1063–1075
46. Heyman, N. S., Kurjiaka, D. T., Ek Vitorin, J. F., and Burt, J. M. (2009) *Am. J. Physiol. Heart Circ. Physiol.* **297,** H450–H459
47. Hur, K. C., and Louis, C. F. (1989) *Biochim. Biophys. Acta.* **1010,** 56–63
48. Mathias, R. T., Kistler, J., and Donaldson, P. (2007) *J. Membr. Biol.* **216,** 1–16